A Compact Dual-Polarized Wideband Patch Antenna Array for the Unlicensed 60 GHz Band

Frank Wollenschläger[1], Ralf Stephan[2], Lei Xia[3], Jens Müller[4], Robert Müller[5], Alexis Paolo Garcia Ariza[6], Reiner S. Thomä[7], and Matthias A. Hein[8]

[1-8]*Institute for Micro- and Nanotechnologies, Ilmenau University of Technology, P.O.Box 10 05 65, 98684 Ilmenau, Germany*
[1-8]*{frank.wollenschlaeger, ralf.stephan, lei.xia, jens.mueller, mueller.robert, alexis-paolo.garcia-ariza, reiner.thomae, matthias.hein}@tu-ilmenau.de*

***Abstract*— The unlicensed 60 GHz industrial, scientific and medical (ISM) radio band provides a wide bandwidth for wireless high data rate communication systems. To optimally utilize these millimeter wave data transmission channels, exploiting orthogonal polarizations is a crucial enhancement. Along with the increase in data rate, improvements of the robustness of communication links in wireless local/personal area networks (WLANs/WPANs) can be achieved adopting the dual-polarization approach. Adjustment of the proper antenna gain is essential for meeting a specific link budget. We have designed, fabricated, and characterized a patch antenna array utilizing orthogonal polarizations in planar multilayer technology.**

I. Introduction

The international unlicensed 60 GHz ISM-band provides up to 9 GHz instantaneously available bandwidth, to provide high data rates in wireless links over moderate distances [1]. The design of a wideband antenna is a crucial prerequisite for such applications. Although most existing research activities concentrate on linearly polarized approaches, the utilization of dual polarizations can almost double the data rates, reduce the fading margins of the wireless transmission channels, and compensate for polarization misalignment.

Another benefit of dual-polarized antennas is channel sounding for the extraction of polarimetric channel information. To thoroughly characterize a time-variant wireless communication channel, real-time acquisition of data is mandatory. While acquiring data for both polarizations sequentially is possible, in general, a simultaneous approach is preferable, although at the expense of higher frontend complexity [2]. The antenna proposed here was specifically designed for such real-time channel sounding at millimeter-wave frequencies.

The packaging technology is another important aspect of the integration of millimeter-wave antennas in conjunction with integrated circuits (MMICs), transmission line based elements like filters or couplers, and ancillary electronic devices. We have applied the low-temperature co-fired ceramics (LTCC) technology, which offers a truly three-dimensional integration of microwave structures and features low dielectric losses at millimeter wave frequencies [3].

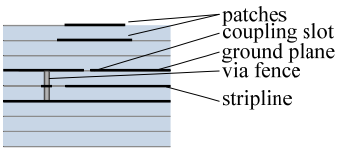

Fig.1: Layer stack of one patch element. The antenna requires at least five dielectric layers as indicated and is implemented on an eight-layer substrate.

II. Antenna Design

A. Basic antenna element

The antenna was designed to cover most of the 60 GHz ISM-band, more specifically 59.5 to 66.5 GHz [2]. To benefit from future improvements of MMIC technology and performance, and to offer some robustness against fabrication tolerances, larger bandwidths are always preferable.

To provide an antenna structure that offers a good compatibility with the quasi-planar LTCC process, patch antennas were chosen. While for earlier work, arrays of basic patch elements were sufficient [4, 5], a more elaborated design with stacked patches was applied here, to meet the required wide impedance bandwidth. A similar approach with microstrip feed and limited to linear polarization was adopted in [6]. Fig. 1 sketches the layer stack of a single antenna element, fed by aperture coupling. The patch sizes and their geometrical arrangements were optimized by electromagnetic full-wave simulation using Ansoft HFSS [7]. For the coupling slot, a rectangular shape yielded the best results over dog-bone and H-shaped slot geometries. For the simulation model of the slot, the corners were rounded, to better match the structure resulting after manufacturing. The slot is not centered below the patches, but displaced by an offset along the smaller dimension of the patch. Although this design is disadvantageous in terms of the coupling between the slot and the patches, it leaves the currents on the ground plane flow less distorted by the relatively large aperture, and thus improves the gain of the antenna element. The reduced

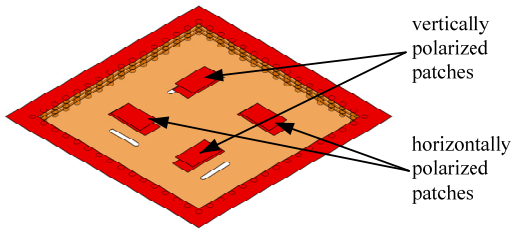

Fig.2: 2×2 patch array configuration. Each pair of diagonally located patches radiates in one polarization as indicated in the figure.

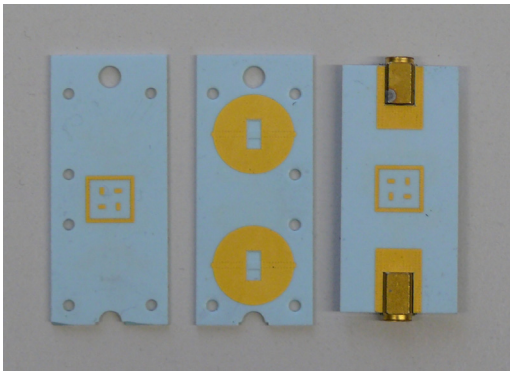

Fig.3: Photographs of the antenna test substrates manufactured for measurement. On the left-hand side, a top view of an antenna with waveguide feed is shown; the corresponding backside is shown in the center panel. On the right-hand side, an antenna outfitted with MMPX coaxial connectors but otherwise identical patch geometry is displayed.

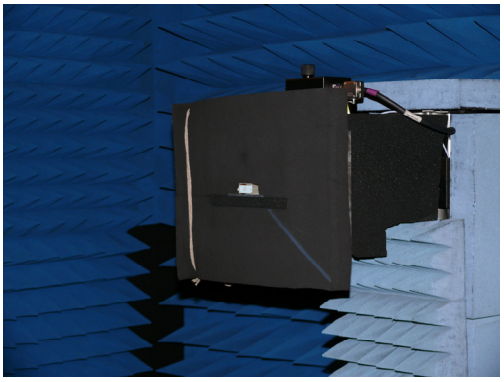

Fig.4: Photograph of the antenna attached to the rotational positioning system inside the anechoic chamber. The antenna is directly connected to the open waveguide junction of the down-converting harmonic mixer. The lower half-space of the antenna is covered by absorber foam and cannot be measured for the waveguide based antenna design.

coupling was compensated for by adjusting a matching stub later on.

The antenna is designed as one part of a dense miniaturized microwave package. To use the smallest possible footprint area for the antenna itself, its feed structure has to be located entirely in buried layers. Hence, striplines were the transmission line type of choice.

As the manufacturing of standard 50 Ω striplines at the desired frequencies would exceed the resolution limits of the LTCC technology achievable at present, a conservative line width of 100 µm was chosen, resulting in a characteristic impedance of 37 Ω instead. The striplines are matched to the coupling slots by open stubs. To prevent the excitation of parallel-plate modes at the ends of the stubs or other discontinuities, all striplines were shielded by via fences. These fences had to be widened around the aperture, to allow for undisturbed current flow along the slot. The resultant cavity behind the slot is still small enough to avoid resonances within the targeted frequency band.

All vias have a diameter if 150 µm and a minimum distance of 350 µm to comply with the technological constraints.

B. Array geometry

To optimally exploit dual polarizations, both orientations have to be fed separately. For example, such an approach enables the excitation of left-handed (LHCP) or right-handed circularly polarized (RHCP) waves, if a 90-degrees phase difference is generated between the two feeds. The approach proposed in [2] incorporates adjustable phase shifters, to facilitate switching between LHCP, RHCP, and linear polarization.

To achieve a sufficiently high cross-polar discrimination (XPD) across the main beam, the radiators for both polarizations have to share a common phase center. Simulations showed that it is impossible to feed a single rectangular patch with both polarizations while still obtaining an acceptable gain as well as the required bandwidth. Thus, an array configuration as displayed in Fig. 2 was chosen. Each pair of diagonally arranged antenna elements is responsible for one polarization, with the common phase center located in the geometric center between the four patches. The distance between the elements of a pair is half of the free-space wavelength at 60 GHz.

As patch antennas on high-permittivity substrates tend to excite surface waves, the entire array is encompassed by a metallic wall consisting of grounded via fences. These walls inhibit the propagation of surface waves across the substrate, reducing unwanted radiation from its edges.

The antenna was designed to be used in conjunction with hybrid-integrated differential MMICs [8] for each polarization channel, with four feeds in total. Further, the antenna was integrated within a package specifically developed for channel measurements [9]. A version with integrated T-junction based baluns was also designed for single-ended MMICs. The balun is explained in greater detail in [5].

C. Antenna measurement

To evaluate the radiation properties of an antenna at 60 GHz by measurement, a special test version with an appropriate wideband transition to the measurement ports had to be designed and manufactured. Earlier work applied coaxial-to-stripline or waveguide-to-microstrip transitions. For the antenna described here, the bandwidth of both approaches was insufficient. Thus, a specific differential WR15 waveguide transition with a –10 dB bandwidth of around 20 GHz has been designed.

The single-ended version of the antenna was also manufactured for testing purposes and outfitted with MMPX type surface-mountable connectors, as illustrated by Fig. 3.

The radiation measurements were performed in the anechoic chamber of Ilmenau University of Technology. Fig. 4. depicts an antenna mounted for pattern measurement on the rotational positioning system in the anechoic chamber of Ilmenau University of Technology. The waveguide-fed module is directly attached to the flange of the down-converter. All metallic surfaces are covered with absorber foam.

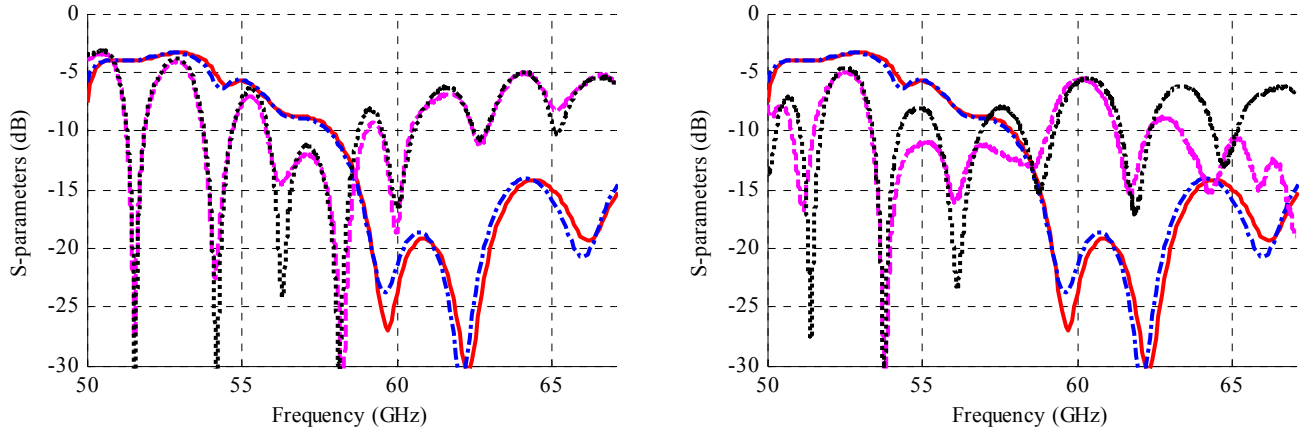

Fig.5: Left-hand side: Simulated (red bold curves) and measured reflection coefficients (blue dash-dotted curves) at port 1, and simulated (black dotted curves) and measured (purple dashed curves) reflection coefficients at port 2 of the waveguide-fed antennas. Right-hand side: Same for the coaxial-fed antennas. For both versions, the deviation of the matched frequency range between measured and simulated results is around 4 GHz. The return loss is higher than 10 dB between 56 and 60.5 GHz for the waveguide fed version, and between 53.5 and 59 GHz for the coaxial-fed version.

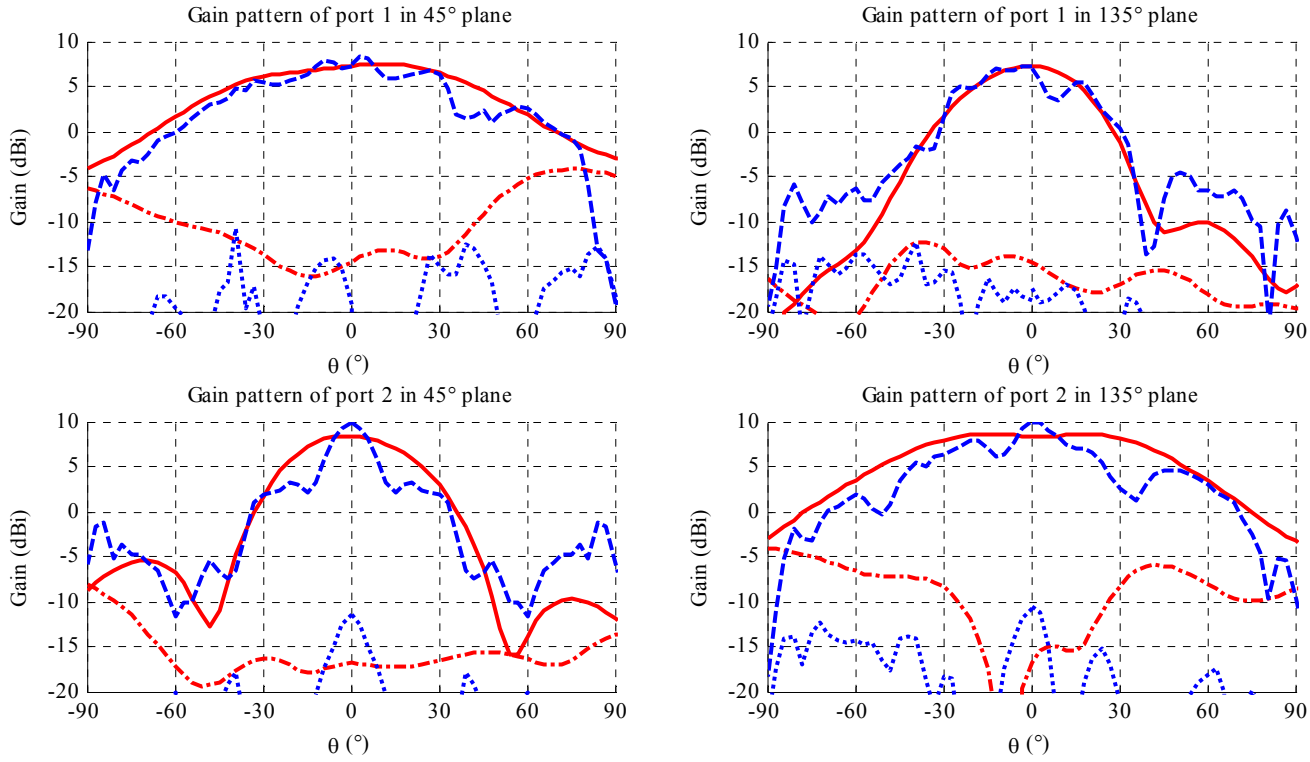

Fig.6: Gain patterns of the waveguide-fed antenna: Simulated (red solid curves) and measured (blue dashed curves) co-polar and simulated (red dash-dotted curves) and measured (blue dotted curves) cross-polar patterns. The measured gain has been corrected for an estimated 1 dB of losses in transition lines and feed cables. The top diagrams depict the pattern of the antenna for feeding at port 1, while the bottom diagrams refer to port 2. The patterns are displayed for azimuth angles of 45° and 135°, corresponding to the planes of minimum and maximum beamwidth.

III. Measurement Results

The antennas including the transition structures were fabricated on DuPont DP943™ tape with gold metallization; a photograph of the test modules fabricated is shown in Fig. 3. The circular contact areas for the waveguide flanges can be seen on the backside of these substrates (center panel). For the version with coaxial connectors, a solderable layer was added. The complex-valued dielectric properties of the LTCC material were derived from separate measurements and found to amount to $\varepsilon \approx 7.54$ and $\tan\delta \approx 0.003$ [10].

The S-parameters were measured with an Agilent E8361A vector network analyzer. The results are displayed in Fig. 5. The coupling between the ports was measured for the coaxial feed lines only and was below –30 dB for the entire operating frequency band of the antenna. A good decoupling between the channels is especially important for calibration, for channel sounding. The layout of the waveguide transition did

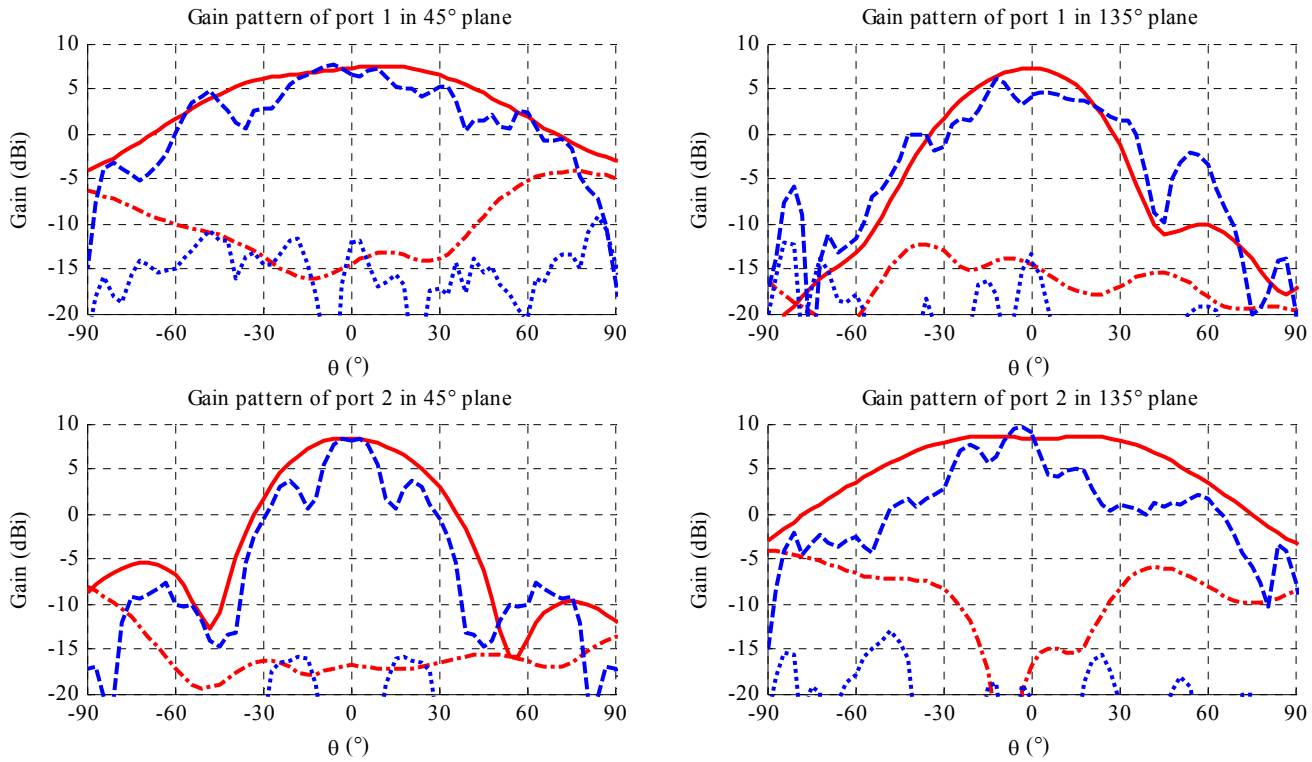

Fig.7: Gain patterns of the coaxial-fed antenna: Simulated (bold red solid curves) and measured (bold blue dashed curves) co-polar and simulated (red dash-dotted curves) and measured (blue dotted curves) cross-polar patterns. The measured gain has been corrected for an estimated 3 dB of losses in transition lines, feed cables, and adapters.

not enable a transmission measurement for the corresponding modules but is expected to yield comparable results. For both versions, the measured return loss exhibits a frequency shift with respect to the simulated values, which is attributed to a geometric deviation of the manufactured matching stubs from the design values. The waveguide-equipped antennas display a return loss of more than 10 dB between 56 and 60.5 GHz, resulting in a fractional bandwidth of 7.5%. The coaxial-fed counterpart exhibits a fractional bandwidth of 9.8%, between 53.5 and 59 GHz.

The results of the gain pattern measurements are displayed in Fig. 6 and Fig. 7. The patterns of both types of antennas exhibit a maximum and a minimum of the beamwidth in the 45°- and the 135°-planes, depending on the feed port. The shape of the beam is a result of the diagonal arrangement of the two pairs of orthogonally polarized patches.

For both versions, all gain patterns display a certain ripple which can be attributed to remaining surface waves that radiate from the edges of the test substrates. Apart from this effect, the simulated and measured patterns match well, with a maximum gain of about 7.5 dBi, resulting in a radiation efficiency between 60 and 65% within the target frequency band. At 60 GHz, the XPD was found to be better than 10 dB within the 3-dB beamwidth, and better than 20 dB within the narrower minimum 3-dB beamwidth of 35°.

IV. Conclusions

A dual polarized antenna for wireless high data rate transmission and channel sounding measurements was designed. Two versions of the antenna were manufactured for experimental characterization of scattering parameters and radiation patterns. One realization was fed by a waveguide-to-stripline transition and exhibited an impedance bandwidth of 7.5%, while the second design included a coaxial connector and yielded a fractional bandwidth of 9.8%. Both versions exhibit a gain of approximately 7.5 dBi, after accounting for transition losses, with a minimum 3-dB beamwidth of 35°, and a cross-polar discrimination of more than 20 dB.

Both versions are planned to be integrated into an LTCC module specifically tailored to polarimetric wideband microwave channel measurement purposes.

Acknowledgment

This work has been funded by the German Ministry of Education and Research through subcontracts from IMST GmbH and IHP GmbH in the framework of the R&D-initiative "Enablers for Ambient Systems" (EASY-A) [11]. The authors appreciate very much technical assistance from Michael Huhn, Matthias Zocher, and the colleagues at the Center for Micro- and Nanotechnologies (ZMN).

References

[1] P. F. M. Smulders, "Exploiting the 60 GHz band for local wireless multimedia access: prospects and future directions," *IEEE Commun. Mag.*, Vol. 40, No. 1, pp. 140–147, 2002.

[2] A.P. Garcia Ariza, R. Müller, F. Wollenschläger, L. Xia, M. Elkhouly, Y. Sun, U. Trautwein, R.S. Thomä, "Dual-Polarized Architecture for Channel Sounding at 60 GHz with Digital/Analog Phase Control based on 0.25µm SiGe BiCMOS and LTCC Technology", *The 5th European*

Conference on Antennas and Propagation – EuCAP 2011, Rome, Italy, April 2011.

[3] J.F. Trabert, K.H. Drüe, J. Müller, R.A. Perrone, R. Stephan, M.A. Hein, "High-performance 3-dimensional hybrid-integrated switch matrix for Ka-band satellite communication application based on ceramic multilayer technology", *IMAPS 2007*, San Jose, CA, USA, Nov. 2007.

[4] A.E.I. Lamminen, J. Saily, A.R. Vimpari, "60 GHz Patch Antennas and Arrays on LTCC with Embedded-Cavity Substrates", *IEEE Trans. Antennas Propag.*, Vol. 56, Issue 9, pp. 2865-2874, Sep. 2008.

[5] F. Wollenschläger, R. Stephan, L. Xia, J. Müller, M.A. Hein, "A broadband 60 GHz aperture-coupled patch array integrated in multilayer ceramics technology", *International Conference on Electromagnetics and Advanced Applications – ICEAA 2010*, Sydney, Australia, Sep. 2010.

[6] Shenario Ezhil Valavan. A, Bill Yang, Alexander Yarovoy, L.P. Ligthart, "An M-Band Differentially Fed, Aperture Coupled Stacked Patch Antenna in LTCC", *Proceedings of the 5th European Radar Conference*, Amsterdam, The Netherlands, Oct. 2008, pp. 200-203.

[7] Ansoft HFSS Website [Online]. Available: http://www.ansoft.com/HFSS/

[8] M. Elkhouly, S. Glisic, C. Scheytt, "A 60 GHz wideband high output P1sB up-conversion image rejection mixer in 0.25 µm SiGe technology", *2010 Topical Meeting on Silicon Monolithic integrated Circuits in RF Systems – SiRF*, Jan. 2010.

[9] R. Müller, A. P. Garcia, L. Xia, F. Wollenschläger, A. Schulz, R. S. Thomä, M. A. Hein, J. Müller, "60 GHz Ultrawideband Hybrid-Integrated Dual-Polarized Front-End in LTCC Technology", *The 5th European Conference on Antennas and Propagation – EuCAP 2011*, Rome, Italy, Apr. 2011.

[10] DuPont Microcircuit Materials: 943 Low Loss Green Tape [Online]. Available: http://www2.dupont.com/MCM/en_US/PDF/datasheets/943.pdf

[11] EASY-A Enablers for Ambient Services & Systems, project website [Online]. Available: http://www.easy-a.de/